JOURNAL OF THEORETICAL
AND APPLIED MECHANICS
52, 2, pp. 507-518, Warsaw 2014

INFLUENCE OF THE ELASTOMERIC COATING ON PARAMETERS OF STEADY STATE VIBRATIONS OF COIL SPRINGS IN THE RESONANCE AND OUTSIDE IT

Krzysztof Michalczyk
AGH University of Science and Technology, Faculty of Mechanical Engineering and Robotics, Krakow, Poland
e-mail: kmichal@agh.edu.pl

The computational model of steady state vibrations of the coil spring covered with an elastomeric layer under resonance conditions and outside them is presented in the paper. It enables one to assess the reduction effectiveness of dynamic stresses in function of the material and geometrical parameters of the applied coating. The considerations are supplemented with the numerical examples.

Keywords: helical springs vibrations, coil springs, dynamic stresses, damping

1. Introduction

Coil springs due to their reliability, wide stiffness range, resistance to unfavourable work conditions and time invariable force-strain characterisics, constitute the most popular elastic coupling links. Coil springs used in machines generating high frequency or not harmonic excitations are often exposed to operations in a circum-resonant range (Branowski, 1997). Studies aimed at a reduction of natural vibrations of valve springs in internal combustion engines, carried out through many years, indicate the importance of this problem (Flenker and Uphoff, 2005; Liu and Kim, 2009; Yang *et al.*, 1996; FIAT – Bollettino Tecnico, 1962). These vibrations cause dynamic stresses in valve springs of the reduced values reaching up to approxmately 2000 MPa (Muhr, 1993). An additional unfavourable effect accompanying natural vibrations is – in this case – the valve loss of tightness, which can lead to a serious engine failure. Natural vibrations constitute also a problem of springs used in suspension systems of automotive and rail-vehicles (Dickhart and Herring, 1985). Propagation of vibrations of audio and higher frequencies in automotive vehicles can cause material strengthening in welded and annealed joints, negatively influencing their fatigue strength (Boschi, 1961). Coil springs can buckle already at a very low slenderness ratio (Krużelecki, 1990) – natural vibrations of springs caused by local stiffness changes can significantly contribute to their stability loss. These vibrations can reach high amplitudes in coil springs due to very low damping properties of steels used, most often during their production. As it was experimentally indicated and presented by Michalczyk (2012), for the usually applied mounting methods of coil springs, the ability to dissipate energy in the system: spring – mounting element, expressed by means of the logarithmic damping decrement, usually does not exceed 0.001. It was shown in the paper by Michalczyk and Majkut (2003) that circum-resonant ranges of the maximum forces increase in springs much wider than the ranges of increasing vibration amplitudes of the vibroinsulated mass, which encompases only the close vicinity of the system resonance frequency. It was also pointed out that these forces are getting higher and higher values in the successive valleys between resonances. Very weak damping properties of coil springs are the reason of searching for solutions which would allow one to increase the dissipation of energy collected in coil springs. There are several methods increasing damping in the spring-mounting element system. In these solutions, either a dry friction between the coils and mounting elements is applied (Shulgin and Sjemionov, 1985; Mayers, 1985) or elastomers of high damping capability are used in the spring mounting elements (Nix, 2001; Boschi, 1961; Michalczyk and Michalczyk, 2009). The strength analysis and investigations concerning damping properties of the solution presented by Michalczyk and Michalczyk (2009), were shown in Michalczyk and Lepiarczyk (2011) and Michalczyk (2012). The classic example of the reduction of natural vibrations of coil springs is the application of multi-wire coil springs in machine guns recuperators, e.g. in the Kalashnikov rifle (Clark, 1961; Costello and Philips, 1979; Żukowski, 1955). Another way of increasing damping in the system of the spring and mounting element is an application of elastomeric coatings on the coil wires. This solution was presented by Muzio (1998) and Nishiyama *et al.* (1988). However, the lack of computational methods allowing one to determine the coating effectiveness in relation to its parameters, prevented a wider application of this solution. The analysis of effectiveness of the limiting maximum stresses caused by longitudinal vibrations of the coil springs subjected to excitations of resonance frequences was presented by Michalczyk (2013). The model given by Michalczyk and Majkut (2003) allows one to determine the damping effectiveness of the elastomeric coating covering the total coil wire length solely under the resonance condition.

The aim of the present paper is development of the model enabling determination of parameters of longitudinal damped vibrations of a spring covered with an elastomeric coating in the whole range of excitation frequencies.

2. Analysis

The model of the spring subjected to forced excitation, modified in a way suitable for calculations in the case of excitations of a kinematic character, was applied in this study. The analysed system is presented in Fig. 1.

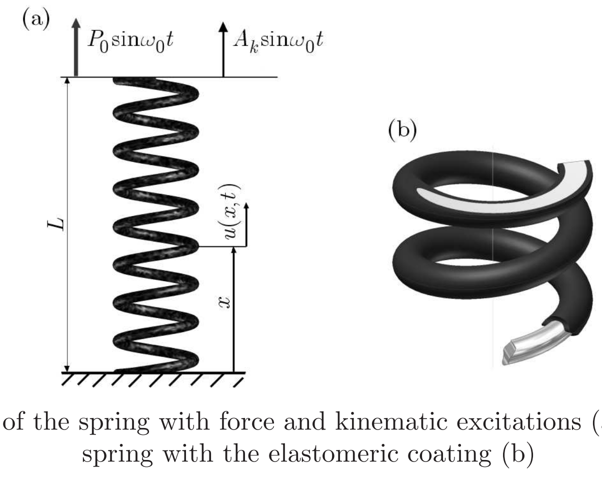

Fig. 1. Analysed model of the spring with force and kinematic excitations (a), sector of the analysed spring with the elastomeric coating (b)

The classic model of the equivalent rod was used in considerations (similarly as in Michalczyk (2013)) since, as it was shown in Pietra and Valle (1982), the spring model developed by Wittrick (1966), taking into account the coupling between longitudinal and torsional vibrations, provides – for typical springs – only insignificantly more accurate results than the classic model. This model has the equivalent stiffness EA, equivalent linear density ρA, and equivalent damping coefficient αA. The effects of the end coils preparation and the way of mounting them were neglected in the analysis as these effects are significant only with regards to springs with a very small number of acting coils (Michalczyk and Salwiński, 2011). It was also assumed that the analysis concerns only these cases in which there is no risk of the loss of stability. The wave equation of the rod longitudinal vibrations, taking into account the internal damping modelled by viscous damping depending on the excitation frequency and a continuous loading of the amplitude given by the function $q_0(x)$ has the form

$$EA\frac{\partial^2 u}{\partial x^2} + \alpha A\frac{\partial^3 u}{\partial x^2 \partial t} - \rho A\frac{\partial^2 u}{\partial t^2} = -q_0(x)\sin\omega_0 t \tag{2.1}$$

The right side of equation (2.1) $q_0(x)\sin\omega_0 t$ represents the external longitudinal continuous load acting on the spring. The equivalent compression rigidity for the spring of the wire covered by the elastomeric layer according to (Michalczyk, 2013) equals

$$EA = \frac{[(GJ)_s + (GJ)_e]L}{\pi R^3 n\cos\gamma} \tag{2.2}$$

(2.2) where $(GJ)_{s,e}$ is the product of the shear modulus of elasticity and the axial moment of inertia for the wire (index: s) or for the elastomeric coating (index: e), L – initial spring working height, R – nominal spring radius, n – number of working coils, γ – pitch angle.

The equivalent linear density equals

$$\rho A = \frac{n\pi^2 R}{2L\cos\gamma}[d_s^2\rho_s + (d_e^2 - d_s^2)\rho_e] \tag{2.3}$$

where d_s is the diameter of the coil wire, d_e – diameter of the elastomeric coating, ρ_s – density of the wire material, ρ_s – density of the elastomeric coating material.

The equivalent specific damping capacity can be calculated from the condition of the equality of the dissipated energy for one vibration period in the material and due to viscous damping

$$dL_{Tm} = dL_{Tw} \tag{2.4}$$

In order to do this, we will consider the equivalent rod sector of length dx performing harmonic vibrations in accordance with the equation: $u(x,t) = X(x)\sin\omega_0 t$. For the viscous damping model, the longitudinal force in the equivalent rod is expressed by

$$F = F_s + F_d = EA\varepsilon + \alpha A\dot{\varepsilon} \tag{2.5}$$

The energy loss by viscous damping for the vibration period is

$$dL_{Tw} = \int\limits_0^T dN_t\,dt = \int\limits_0^{2\pi/\omega_0} \alpha A\dot{\varepsilon}^2 dx\,dt \tag{2.6}$$

where

$$\dot{\varepsilon} = \frac{\partial}{\partial t}\Big(\frac{\partial u}{\partial x}\Big) = \frac{\partial}{\partial t}(X'\sin\omega_0 t) = \omega_0 X'\cos\omega_0 t \tag{2.7}$$

Thus substituting (2.7) into (2.6)

$$dL_{Tw} = \alpha A\omega_0\pi X'^2 dx \tag{2.8}$$

The work of the elasticity force of the maximum value $F_{s\,MAX}$

$$dL_S = \frac{F_{s\,MAX}^2}{2EA}dx = \frac{(EA)^2 X'^2}{2EA}dx \tag{2.9}$$

thus, the work of internal damping will be

$$dL_{Tm} = \psi dL_S = \psi\frac{(EA)^2 X'^2}{2EA}dx = \frac{1}{2}\psi EAX'^2 dx \tag{2.10}$$

where ψ is the equivalent specific damping capacity

$$\psi = \frac{\psi_s(EA)_s + \psi_e(EA)_e}{(EA)_s + (EA)_e} \tag{2.11}$$

This coefficient for the given material is defined as the ratio of the loss of energy during one period of vibrations, measured by a hysterises loop area, to the energy corresponding to the amplitude of the strain expressed by means of a triangle area (Lipiński, 1985).

Substituting (2.8) and (2.10) into (2.4) and rearanging, we finally obtain

$$\alpha A = \frac{\psi EA}{2\pi\omega_0} \tag{2.12}$$

We are looking for the solution to (2.1) in form of a series

$$u(x,t) = \sum_{i=1}^{\infty} X_i(x)T_i(t) \tag{2.13}$$

where $X_i(x)$ are successive functions of natural vibrations, $T_i(t)$ – time functions (being looked for). The separation of variables is possible due to distribution of the constant load amplitude $q_0(x)\sin\omega_0 t$ into the eigenfunction series

$$q_0(x) = \sum_{i=1}^{\infty} h_i X_i(x) \tag{2.14}$$

The balance coefficient h_i can be determined using the orthogonality of eigenfunctions. Multiplying bilaterally dependence (2.14) by an arbitrary term from the series X_j and integrating bilaterally from 0 to L, where L is the working spring height, we obtain

$$\int_0^L q_0(x)X_j(x)\;dx = \sum_{i=1}^{\infty} h_i \int_0^L X_j(x)X_i(x)\;dx = h_{i=j}\int_0^L X_{i=j}^2(x)\;dx \tag{2.15}$$

From here, in the general case (Solecki and Szymkiewicz, 1964)

$$h_i = \frac{\int_0^L q_0(x)X_i(x)\;dx}{\int_0^L X_i^2(x)\;dx} \tag{2.16}$$

For the case when loading $q_0(x)$ is given in a form of a concentrated force P_0 applied to the rod end (Fig. 1a), dependence (2.16) rearranges itself into the form (Giergiel, 2000)

$$h_i = \frac{P_0 X_i(L)}{\int_0^L X_i^2(x)\;dx} \tag{2.17}$$

Substituting (2.14) and partial derivatives (2.13) into equation (2.1), we obtain for the arbitrary i-th term of the series

$$EAX_i''T_i + \alpha AX_i''\dot{T}_i - \rho AX_i\ddot{T}_i = -h_iX_i\sin\omega_0 t \tag{2.18}$$

then transferring and dividing the variables. we obtain

$$\frac{X_i''}{X_i} = \frac{\rho A\ddot{T}_i - h_i\sin\omega_0 t}{EAT_i + \alpha A\dot{T}_i} = -\lambda_i^2 \tag{2.19}$$

where λ_i is a certain constant. On the basis of (2.19), we obtain the final forms of the equations of spring motion

$$X_i'' + \lambda_i^2 X_i = 0 \qquad \ddot{T}_i + p_i^2 \frac{\alpha A}{EA}\dot{T}_i + p_i^2 T_i = \frac{h_i}{\rho A}\sin\omega_0 t \tag{2.20}$$

where

$$p_i^2 = \frac{EA}{\rho A}\lambda_i^2 \tag{2.21}$$

In order to determine the values of the balance coefficients h_i, in the series approximating the concentrated force P_0, the successive forms of the natural vibrations should be determined. On the basis of equation $(2.20)_1$, we have

$$X_i(x) = C_{1i}\sin\lambda_i x + C_{2i}\cos\lambda_i x \tag{2.22}$$

and the boundary conditions for the considered free vibrations are

$$X_i(x=0) = 0 \qquad \text{and} \qquad X_i'(x=L) = 0 \tag{2.23}$$

From here $C_{2i} = 0$ and $0 = C_{1i}\lambda_i\cos\lambda_i L$, thus

$$\lambda_i = \frac{2i-1}{2L}\pi \qquad i = 1,2,3,\dots \tag{2.24}$$

Normal modes will be

$$X_i(x) = C_{1i}\sin\Big(\frac{2i-1}{2L}\pi x\Big) \tag{2.25}$$

By substituting (2.25) into (2.17), we obtain

$$h_i = \frac{P_0 C_{1i}\sin\Big(\frac{2i-1}{2}\pi\Big)}{C_{1i}^2\int\limits_0^L \sin^2\Big(\frac{2i-1}{2L}\pi x\Big)\,dx} = \frac{2P_0\sin\Big(\frac{2i-1}{2}\pi\Big)}{C_{1i}L} \tag{2.26}$$

Equation $(2.20)_2$ has the solution in form of a sum of the general integral of the homogeneous solution (describing natural vibrations decaying in time) and the particular integral of the heterogeneous equation (describing the steady state under an influence of the given excitation). Since we are looking for the steady solution, we determine only the particular integral expected in the form

$$T_i(t) = G_{1i}\sin\omega_0 t + G_{2i}\cos\omega_0 t \tag{2.27}$$

Substituting (2.27) together with its derivatives into $(2.20)_2$ and rearranging, we obtain

$$\begin{aligned}&\Big(-G_{1i}\omega_0^2 - p_i^2\frac{\alpha A}{EA}G_{2i}\omega_0 + p_i^2 G_{1i}\Big)\sin\omega_0 t + \Big(-G_{2i}\omega_0^2 - p_i^2\frac{\alpha A}{EA}G_{1i}\omega_0 + p_i^2 G_{2i}\Big)\cos\omega_0 t\\ &\quad = \frac{h_i}{\rho A}\sin\omega_0 t\end{aligned} \tag{2.28}$$

Comparing the coefficients at $\sin\omega_0 t$ and $\cos\omega_0 t$, we finally obtain

$$G_{1i} = \frac{h_i}{\rho A}\frac{p_i^2-\omega_0^2}{(p_i^2-\omega_0^2)^2 + p_i^4\Big(\frac{\alpha A}{EA}\Big)^2\omega_0^2} \qquad G_{2i} = \frac{-h_i}{\rho A}\frac{p_i^2\frac{\alpha A}{EA}\omega_0}{(p_i^2-\omega_0^2)^2 + p_i^4\Big(\frac{\alpha A}{EA}\Big)^2\omega_0^2} \tag{2.29}$$

Substituting (2.29) into (2.27), we obtain

$$T_i(t) = \frac{h_i}{\rho A}\frac{p_i^2-\omega_0^2}{(p_i^2-\omega_0^2)^2+p_i^4\Big(\frac{\alpha A}{EA}\Big)^2\omega_0^2}\sin\omega_0 t + \frac{h_i}{\rho A}\frac{-p_i^2\frac{\alpha A}{EA}\omega_0}{(p_i^2-\omega_0^2)^2+p_i^4\Big(\frac{\alpha A}{EA}\Big)^2\omega_0^2}\cos\omega_0 t \tag{2.30}$$

The steady-state solution to equation (2.1) in accordance with (2.13) has the form of the sum of products (2.25) and (2.30)

$$\begin{aligned} u(x,t) &= \sum_{i=1}^{\infty} C_{1i}\sin\Big(\frac{2i-1}{2L}\pi x\Big)\\ &\cdot\left(\frac{\frac{h_i}{\rho A}(p_i^2-\omega_0^2)}{(p_i^2-\omega_0^2)^2+p_i^4\Big(\frac{\alpha A}{EA}\Big)^2\omega_0^2}\sin\omega_0 t + \frac{-\frac{h_i}{\rho A}p_i^2\frac{\alpha A}{EA}\omega_0}{(p_i^2-\omega_0^2)^2+p_i^4\Big(\frac{\alpha A}{EA}\Big)^2\omega_0^2}\cos\omega_0 t\right) \end{aligned}\tag{2.31}$$

Substituting h_i by expression (2.26) and simplifying, we obtain

$$\begin{aligned} u(x,t) &= \sum_{i=1}^{\infty}\left(\sin\Big(\frac{2i-1}{2L}\pi x\Big)\frac{2P_0\sin\Big(\frac{2i-1}{2}\pi\Big)}{L\rho A\Big[(p_i^2-\omega_0^2)^2+p_i^4\Big(\frac{\alpha A}{EA}\Big)^2\omega_0^2\Big]}\right.\\ &\left.\cdot\Big[(p_i^2-\omega_0^2)\sin\omega_0 t - p_i^2\frac{\alpha A}{EA}\omega_0\cos\omega_0 t\Big]\right) \end{aligned}\tag{2.32}$$

The spring longitudinal deformations will assume the form

$$\begin{aligned} \varepsilon(x,t) &= \frac{\partial u(x,t)}{\partial x} = \sum_{i=1}^{\infty}\left(\pi\frac{2i-1}{2L}\cos\Big(\frac{2i-1}{2L}\pi x\Big)\frac{2P_0\sin\Big(\frac{2i-1}{2}\pi\Big)}{L\rho A\Big[(p_i^2-\omega_0^2)^2+p_i^4\Big(\frac{\alpha A}{EA}\Big)^2\omega_0^2\Big]}\right.\\ &\left.\cdot\Big[(p_i^2-\omega_0^2)\sin\omega_0 t - p_i^2\frac{\alpha A}{EA}\omega_0\cos\omega_0 t\Big]\right) \end{aligned}\tag{2.33}$$

Equations (2.32) and (2.33) allow one to determine displacements and deformations of the spring subjected to forced loading. In order to find deformations of the spring subjected to kinematic loading (as it is shown on the right side of Fig. 1a), we have to find the dependence between the displacements amplitude A_k for $x = L$ and the amplitude of the excitation force P_0 applied at the spring end. Substituting in (2.32) $x = L$ and rearranging, we obtain

$$u(L,t) = \sum_{i=1}^{\infty}\frac{2P_0}{L\rho A}\left(\frac{(p_i^2-\omega_0^2)\sin^2\Big(\frac{2i-1}{2}\pi\Big)}{(p_i^2-\omega_0^2)^2+p_i^4\Big(\frac{\alpha A}{EA}\Big)^2\omega_0^2}\sin\omega_0 t + \frac{-p_i^2\frac{\alpha A}{EA}\omega_0\sin^2\Big(\frac{2i-1}{2}\pi\Big)}{(p_i^2-\omega_0^2)^2+p_i^4\Big(\frac{\alpha A}{EA}\Big)^2\omega_0^2}\cos\omega_0 t\right) \tag{2.34}$$

To simplify the notation, let us mark the terms from (2.34) by

$$K_{Si} = \frac{(p_i^2-\omega_0^2)\sin^2\Big(\frac{2i-1}{2}\pi\Big)}{(p_i^2-\omega_0^2)^2+p_i^4\Big(\frac{\alpha A}{EA}\Big)^2\omega_0^2} \qquad K_{Ci} = \frac{-p_i^2\frac{\alpha A}{EA}\omega_0\sin^2\Big(\frac{2i-1}{2}\pi\Big)}{(p_i^2-\omega_0^2)^2+p_i^4\Big(\frac{\alpha A}{EA}\Big)^2\omega_0^2} \tag{2.35}$$

In accordance with these new denotations, equation (2.34) can be written as follows

$$u(L,t) = \sum_{i=1}^{\infty}\frac{2P_0}{L\rho A}(K_{Si}\sin\omega_0 t + K_{Ci}\cos\omega_0 t) \tag{2.36}$$

Rearranging

$$u(L,t)=\frac{2P_0}{L\rho A}\sqrt{\Big(\sum_{i=1}^{\infty}K_{Si}\Big)^2+\Big(\sum_{i=1}^{\infty}K_{Ci}\Big)^2}$$
$$\cdot\left(\frac{\sum\limits_{i=1}^{\infty}K_{Si}}{\sqrt{\Big(\sum\limits_{i=1}^{\infty}K_{Si}\Big)^2+\Big(\sum\limits_{i=1}^{\infty}K_{Ci}\Big)^2}}\sin\omega_0 t+\frac{\sum\limits_{i=1}^{\infty}K_{Ci}}{\sqrt{\Big(\sum\limits_{i=1}^{\infty}K_{Si}\Big)^2+\Big(\sum\limits_{i=1}^{\infty}K_{Ci}\Big)^2}}\cos\omega_0 t\right) \tag{2.37}$$

The terms at $\sin\omega_0 t$ and $\cos\omega_0 t$ meet conditions allowing one to assume that they are cosines and sines of a certain angle δ_k. Writing

$$A_k=\frac{2P_0}{L\rho A}\sqrt{\Big(\sum_{i=1}^{\infty}K_{Si}\Big)^2+\Big(\sum_{i=1}^{\infty}K_{Ci}\Big)^2} \tag{2.38}$$

and

$$\cos\delta_k=\frac{\sum\limits_{i=1}^{\infty}K_{Si}}{\sqrt{\Big(\sum\limits_{i=1}^{\infty}K_{Si}\Big)^2+\Big(\sum\limits_{i=1}^{\infty}K_{Ci}\Big)^2}}$$
$$\sin\delta_k=\frac{\sum\limits_{i=1}^{\infty}K_{Ci}}{\sqrt{\Big(\sum\limits_{i=1}^{\infty}K_{Si}\Big)^2+\Big(\sum\limits_{i=1}^{\infty}K_{Ci}\Big)^2}} \tag{2.39}$$

Equation (2.34) can be written in the following form

$$u(L,t)=A_k\sin(\omega_0 t+\delta_k) \tag{2.40}$$

Equations (2.32) and (2.33) can be written in a similar form, however this form is not suitable for numerical calculations. From equation (2.38), it is possible to read directly the excitation force amplitude P_0 as function of the amplitude of the spring end displacement A_k. Returning to the initial notations

$$P_0=\frac{A_kL\rho A}{2\sqrt{\left(\sum\limits_{i=1}^{\infty}\frac{(p_i^2-\omega_0^2)\sin^2\left(\frac{2i-1}{2}\pi\right)}{(p_i^2-\omega_0^2)^2+p_i^4\left(\frac{\alpha A}{EA}\right)^2\omega_0^2}\right)^2+\left(\sum\limits_{i=1}^{\infty}\frac{-p_i^2\frac{\alpha A}{EA}\omega_0\sin^2\left(\frac{2i-1}{2}\pi\right)}{(p_i^2-\omega_0^2)^2+p_i^4\left(\frac{\alpha A}{EA}\right)^2\omega_0^2}\right)^2}} \tag{2.41}$$

thus, equation (2.41) can be substituted into equations (2.32) and (2.33), obtaining thereby the model with the kinematic excitation (Fig. 1a)

$$
\begin{aligned}
u(x,t) &= \frac{A_k}{\sqrt{\left(\sum\limits_{i=1}^{\infty}\frac{(p_i^2-\omega_0^2)\sin^2\left(\frac{2i-1}{2}\pi\right)}{(p_i^2-\omega_0^2)^2+p_i^4\left(\frac{\alpha A}{EA}\right)^2\omega_0^2}\right)^2+\left(\sum\limits_{i=1}^{\infty}\frac{-p_i^2\frac{\alpha A}{EA}\omega_0\sin^2\left(\frac{2i-1}{2}\pi\right)}{(p_i^2-\omega_0^2)^2+p_i^4\left(\frac{\alpha A}{EA}\right)^2\omega_0^2}\right)^2}} \\
&\cdot\sum_{i=1}^{\infty}\left(\frac{\sin\left(\frac{2i-1}{2L}\pi x\right)\sin\left(\frac{2i-1}{2}\pi\right)}{(p_i^2-\omega_0^2)^2+p_i^4\left(\frac{\alpha A}{EA}\right)^2\omega_0^2}\left((p_i^2-\omega_0^2)\sin\omega_0 t-p_i^2\frac{\alpha A}{EA}\omega_0\cos\omega_0 t\right)\right) \\
\varepsilon(x,t) &= \frac{A_k}{\sqrt{\left(\sum\limits_{i=1}^{\infty}\frac{(p_i^2-\omega_0^2)\sin^2\left(\frac{2i-1}{2}\pi\right)}{(p_i^2-\omega_0^2)^2+p_i^4\left(\frac{\alpha A}{EA}\right)^2\omega_0^2}\right)^2+\left(\sum\limits_{i=1}^{\infty}\frac{-p_i^2\frac{\alpha A}{EA}\omega_0\sin^2\left(\frac{2i-1}{2}\pi\right)}{(p_i^2-\omega_0^2)^2+p_i^4\left(\frac{\alpha A}{EA}\right)^2\omega_0^2}\right)^2}} \\
&\cdot\sum_{i=1}^{\infty}\left(\frac{\pi\frac{2i-1}{2L}\cos\left(\frac{2i-1}{2L}\pi x\right)\sin\left(\frac{2i-1}{2}\pi\right)}{(p_i^2-\omega_0^2)^2+p_i^4\left(\frac{\alpha A}{EA}\right)^2\omega_0^2}\left((p_i^2-\omega_0^2)\sin\omega_0 t-p_i^2\frac{\alpha A}{EA}\omega_0\cos\omega_0 t\right)\right)
\end{aligned}
\tag{2.42}
$$

Dependence $(2.42)_2$ can already be used for the determination of the maximum tangential stresses in the spring wire

$$
\tau_s = \frac{\varepsilon(x,t)(EA)_s R\cos\gamma}{(J_0)_s}(r_{max})_s(K)_s
\tag{2.43}
$$

and in its elastomeric coating

$$
\tau_e = \frac{\varepsilon(x,t)(EA)_e R\cos\gamma}{(J_0)_e}(r_{max})_e(K)_e
\tag{2.44}
$$

where $(J_0)_{s,e}$ is the polar moment of inertia of the spring wire section (index: s) and the elastomeric coating (index: e), respectively, $(r_{max})_{s,e}$ – spring wire radius and elastomeric coating external radius, respectively, K – Wahl's factor

$$
K = \frac{4C-1}{4C-4} + \frac{0.615}{C}
\tag{2.45}
$$

where C is the so-called spring factor expressed by the ratio of the nominal spring diameter to the spring wire external diameter. The remaining notations are the same as in equation (2.2).

The above given relationships allow one to determine the maximum values of the spring tangential stresses for the given excitation frequency. Equations (2.42) have the form of the infinite series, which means that it is not possible to obtain the exact solution in a closed form. However, for practical applications, when applying computer methods, an arbitrary finite number of series terms can be used, in dependence on the required accuracy of the representation of the spring motion and expected excitation frequencies.

3. Numerical examples

The spring of the same parameters as in the paper by Michalczyk (2013) was used in the presented here numerical examples illustrating the derived above relationships. This allows comparison of the computational models presented in both papers. The parameters of the analysed spring are as follows: shear modulus of elasticity of the spring material – 80000 MPa, shear modulus of elasticity of the coating material – 7 MPa, spring wire diameter – 7 mm, elastomeric coating external diameter – 14 mm, steel specific damping capacity – 0.01, elastomer specific damping capacity – 0.7, mass of the spring with coating – 0.7 kg. The kinematic excitation amplitude was assumed as $A_k = 0.01\,\mathrm{m}$, (in accordance with the conditions shown in Fig. 1a). Calculations were performed in the MathCad environment.

The diagrams of deformations $\varepsilon(x,t)$ and displacements $u(x,t)$ for the excitation of the first natural frequency of the clamped-clamped rod are presented in Fig. 2. In these and in further diagrams, the time axis is perpendicular to the figure plane and includes one vibration period T, which allows one to see the total waveforms of displacements and deformations, regardless of phase shifts caused by damping. When comparing diagrams (a), (b) and (c) in Fig. 2, one can notice that if the number of terms used in series $(2.42)_1$ does not significantly influence the displacement waveforms in so far as in the case of deformations, the influence of the number of used terms in $(2.42)_2$ is quite essential. In the successive calculations of series (2.42) and (2.43), the term number $i = 1000$ was assumed.

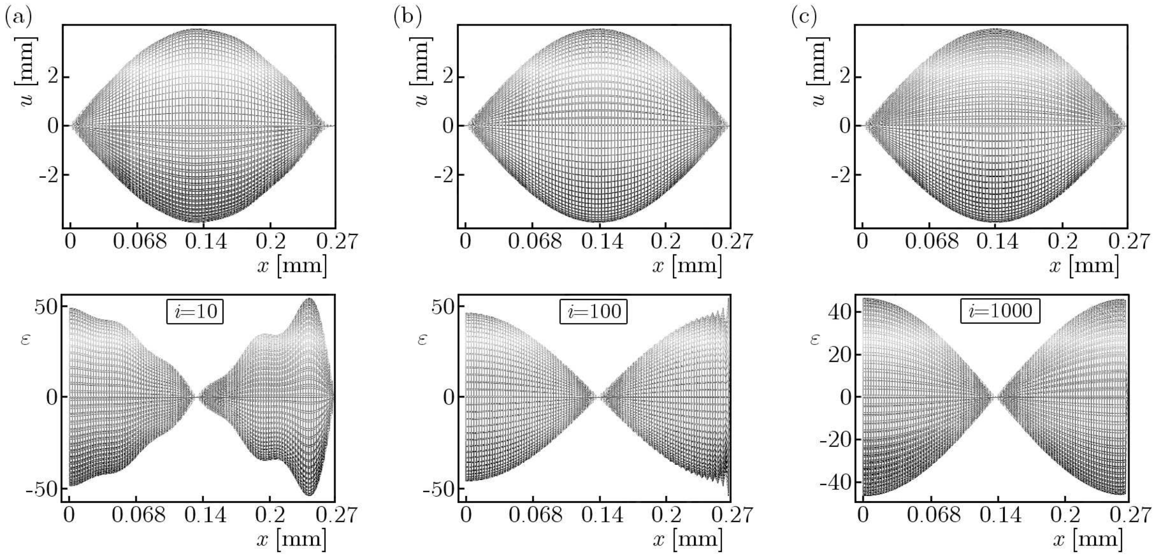

Fig. 2. Sets of diagrams of deformations (upper) and displacements (lower) in the time interval from 0 to T, obtained on the base of (a) equations (2.42) for the first 10 terms of the series, (b) first 100 terms of the series, (c) first 1000 terms of the series at the first natural frequency of the clamped-clamped rod

The expressions derived in the study enabled determination of natural frequencies for the case of the clamped-clamped spring. The comparison of the first three frequencies obtained directly from equation (2.22) for the boundary conditions $X(x = 0) = X(x = L) = 0$ with the values obtained from the simulation, when successively the first 10, 100 and 1000 terms of the series were used in equations (2.42), is presented in Table 1. A difference between the values obtained on the basis of (2.22) and the successive simulations is also presented there. It is seen that already after taking into account the first 100 terms in (2.41) and (2.42) the differences between natural frequencies obtained from the simulation and from equation (2.22) do not exceed 0.2%. For further calculations, $i = 1000$ was assumed.

The distribution sets of the spring tangential stresses in the time interval from 0 to T for the excitation frequency of 1 rad/s and for three successive natural frequencies for the clamped-clamped spring are presented in Fig. 3. When comparing the maximum values of dynamic stresses in Fig. 3b,c,d with static stresses in Fig. 3a, it can be noticed that these values are approximately 1150 times larger. These results, for the given parameters of the system, are in agreement with the results presented in the paper by Michalczyk (2013), where for the same spring parameters the achieved ratio of the resonance dynamic stresses to the static stresses was equal to 1152. This confirms the correctness of the models presented in both the studies.

Table 1

Undamped natural frequencies of the clamped-clamped rod	p_1 [Hz]	p_2 [Hz]	p_3 [Hz]
p_{cal} calculated using equation (2.22)	447.407	894.814	1342.22
p_{sim10} obtained in simulation $(i = 10)$	456.655	913.5	1370.5
$\Delta = 100\%(p_{sim10} - p_{cal})/p_{sim10}$	2%	2%	2%
p_{sim20} obtained in simulation $(i = 100)$	448.32	896.64	1344.95
$\Delta = 100\%(p_{sim100} - p_{cal})/p_{sim100}$	0.2%	0.2%	0.2%
p_{sim30} obtained in simulation $(i = 1000)$	447.52	895.1	1342.6
$\Delta = 100\%(p_{sim1000} - p_{cal})/p_{sim1000}$	0.02%	0.02%	0.02%

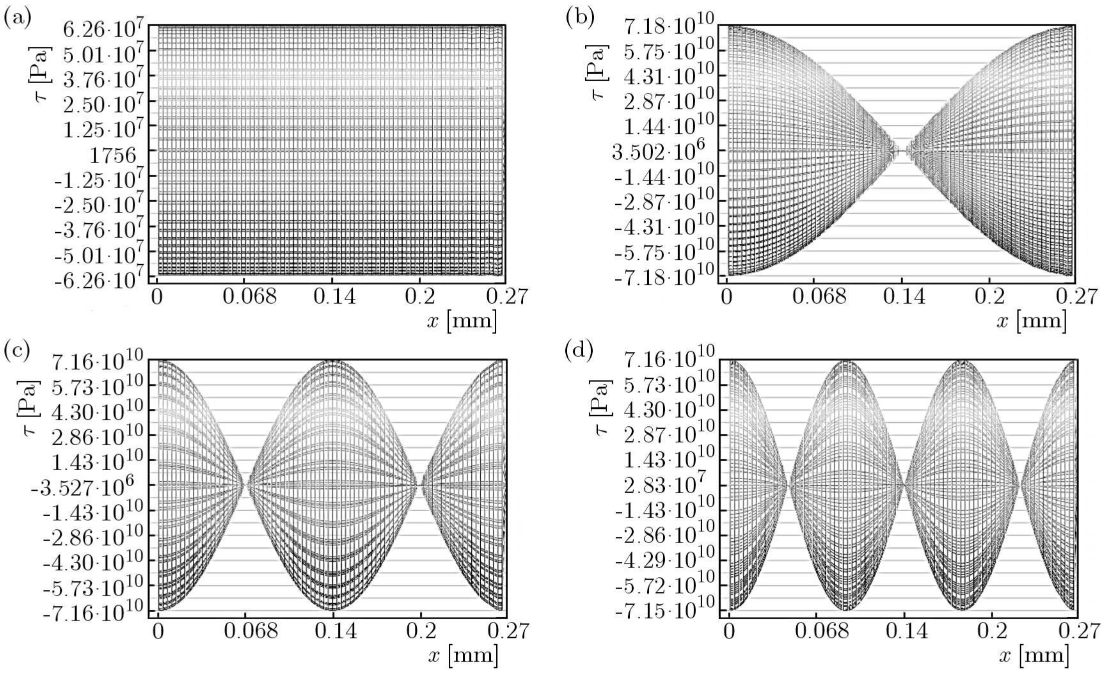

Fig. 3. Sets of diagrams of tangential stresses vs. spring length in the time interval from 0 to T for the excitation frequency of (a) 1 rad/s, (b) 447.52 rad/s, (c) 895.1 rad/s and (d) 1342.6 rad/s

The presented results confirm ow effectiveness of the coatings made of a material having parameters characteristic typical for a industrial rubber in reducing dynamic stresses. The participation of the elastomeric coating in damping is negligible, notwithstanding the fact that the rubber specific damping capacity is approximately 70 times higher than the steel one and that the polar moment of inertia for the elastomeric coating is 15 times larger than for the spring wire section. The reason of such a situation constitutes the low shear modulus of elasticity of the coating material – approximately 11000 times lower than this modulus of the steel of which the springs are made. Thus, the application of a coating material of a higher shear modulus of elasticity with the high specific damping capacity retained, is recommended. These conditions can be met by coatings made out of plastics, e.g. polyethylene (Abdelmouleh *et al.*, 2007).

Diagrams of the maximum tangential stresses τ_s in the spring for three values of the equivalent specific damping capacity $\psi = 0.01, 0.1, 0.3$ at the retained constant equivalent stiffness EA and the equivalent linear stiffness ρA calculated for the above given data and for the same excitation amplitude $(A_k = 0.01\,\mathrm{m})$ are presented in Fig. 4.

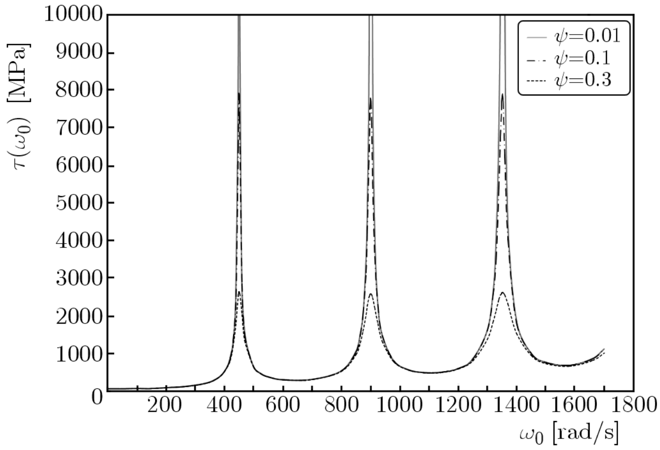

Fig. 4. Maximum tangential stresses in the spring for three different values of the equivalent specific damping capacity ψ

It is seen in Fig. 3a that the tangential stresses value in the considered spring, deflected by 10 mm equals approximately to 63 MPa. Figure 4 indicates that barely for the equivalent specific damping capacity ψ of a value 0.3, the spring resonance dynamic stresses will not exceed 2700 MPa.

4. Conclusions

Equations (2.42), derived in this study, allow one to calculate the parameters of longitudinal vibrations of a spring covered with an elastomeric coating subjected to kinematic excitations. The notation form of these equations allow their easy application by means of numerical methods. These equations together with equations (2.43) and (2.44) enable one to determine the spring state of stresses for an arbitrary excitation frequency. The computational model presented in this paper allows determination of the effectiveness of damping of longitudinal vibrations of the spring covered with a material of high damping properties, thus enabling selection of proper parameters of the coating intended for the given aims. The performed calculations allow one to state that the rubber application as the coating material has a negligible influence on limiting the spring maximum dynamic stresses.

References

1. Abdelmouleh M., Boufi S., Belgacem M.N., Dufresne A., 2007, Short natural-fibre reinforced polyethylene and natural rubber composites: Effect of silane coupling agents and fibres loading, *Composites Science and Technology*, **67**, 1627-1639
2. Boschi A., 1961, *Antivibration Washer for Helical Spring Suspensions*, US 3051469A1
3. Branowski B., 1997, Sprężyny metalowe, PWN, Warszawa
4. Clark H.H., 1961, *Stranded-Wire Helical Springs, Spring Design and Application*, McGraw-Hill Book Company, New York, USA
5. Costello G.A., Phillips J.W., 1979, Static response of stranded-wire helical springs, *International Journal of Mechanical Sciences*, **21**, 171-178
6. Dickhart III W.W., Herring J.J.M., 1985, *Zwischen dem Wagenkasten eines Eisenbahnwagens und einem Drehgestell Angeordnete Mechanische Schraubenfeder*, DE 3529477A1
7. FIAT – Bollettino Tecnico 1962/3, *Alcun note su un caso particolare di vibrazione delle molle*

8. Flenker Ch., Uphoff U., 2005, Efficient valve-spring modelling with MBS valve-train design, *MTZ*, **66**, 12

9. Giergiel J., 2000, *Drgania mechaniczne*, Wydawnictwa AGH, Kraków, p. 397

10. Krużelecki J., 1990, Optimal design of helical springs, *Mechanika Teoretyczna i Stosowana*, **28**, 1/2, 109-114

11. Lipiński J., 1985, *Machines Foundations*, Arkady, Warszawa, p. 33

12. Liu H., Kim D., 2009, Effects of end coils on the natural frequency of automotive engine valve springs, *International Journal of Automotive Technology*, **10**, 4, 413-42

13. Mayers W.T., 1985, *Helical Coil Damper Assemblies*, US 4538563A1

14. Michalczyk K., 2012, The analysis of damping properties of helical spring shock – absorbing holder, *Przegląd Mechaniczny*, **5**, 21-24

15. Michalczyk K., 2013, Analysis of the influence of elastomeric layer on helical spring on its resonant dynamic stresses, caused by its longitudinal vibrations, *Archives of Civil and Mechanical Engineering*, **XIII**, 1, 21-26

16. Michalczyk K., Lepiarczyk D., 2011, Analysis of new construction of amortized handle of coil springs, *Przegląd Mechaniczny*, **70**, 4, 29-32

17. Michalczyk J., Majkut L., 2003, Analysis of wave effects in complex vibration isolation systems, *Archive of Mechanical Engineering*, **L**, 363-385

18. Michalczyk J., Michalczyk K., 2009, *Coil Spring Clamp with the Shock Absorber*, Polish Patent No. PL 387894A1

19. Michalczyk K., Salwiński J., 2011, *Influence of Mounting Way of Helical Compression Spring on its Certain Operating Features* (in Polish), Wydawnictwa AGH, Kraków, p. 72

20. Muhr T.H., 1993, New technologies for engine valve springs, *SAE Paper 930912, New Engine Design and Engine Component Technology, SAE SP-972*, 199-208

21. Muzio C., 1998, *Coated Coil Spring, Particularly for Automotive Suspensions*, EP 0 878637 A2

22. Nishiyama M., Umetsu C., Kebukawa A., Andoh M., 1988, *Coated Coil Spring*, US 4763882

23. Nix S., 2001, *Schubfeder*, DE 10104936A1

24. Pietra L.D, Valle S.D., 1982, On the dynamic behavior of axially excited helical springs, *Meccanica*, **17**, 1, 31-43

25. Shulgin N.M., Sjemionov G.A., 1985, *Ustroistvo dlya kreplenia cilindricheskoi vintovi puzhiny*, SU 12640539A1

26. Solecki R., Szymkiewicz J., 1964, *Układy prętowe i powierzchniowe, obliczenia dynamiczne*, Arkady, Warszawa, p. 65

27. Wittrick W.H., 1966, On elastic wave propagation in helical springs, *International Journal of Mechanical Science*, **8**, 25-47

28. Yang O., Engel P., Prasad B.G.S., Woollatt D., 1966, Dynamic response of compressor valve springs to impact loading, *International Compressor Engineering Conference*, Paper 1131

29. Żukowski S., 1955, *Sprężyny*, PWT, Warszawa, p. 286

Manuscript received January 18, 2013; accepted for print November 19, 2013